Journal of Organometallic Chemistry, 323 (1987) 247–259
Elsevier Sequoia S.A., Lausanne – Printed in The Netherlands

REACTION OF ALKENES WITH *trans*-MeOIr(CO)(PPh_3)$_2$. CRYSTAL AND MOLECULAR STRUCTURE OF THE PENTACOORDINATE ALKOXY-ALKENE IRIDIUM(I) COMPLEX, MeOIr(CO)(PPh_3)$_2$(TCNE)

THOMAS S. JANIK, KAREN A. BERNARD, MELVYN ROWEN CHURCHILL* and JIM D. ATWOOD*

Department of Chemistry, University at Buffalo, State University of New York, Buffalo, New York 14214 (U.S.A.)

(Received October 27th, 1986)

Summary

The reaction of *trans*-MeOIr(CO)(PPh_3)$_2$ with TCNE (tetracyanoethylene) gives rise to the stable adduct MeOIr(CO)(PPh_3)$_2$(TCNE), the structure of which has been determined via a single-crystal X-ray diffraction study. This complex crystallizes in the centrosymmetric orthorhombic space group *Pbca* (D_{2h}^{15}; No. 61) with *a* 17.806(4), *b* 20.769(4), *c* 20.589(6) Å, *V* 7614(3) Å^3 and $Z = 8$. Diffraction data (Mo-K_α, $2\theta = 5–45°$) were collected on a Syntex $P2_1$ automated four-circle diffractometer and the structure was solved and refined to R_F 6.2% for 3502 data with $|F_o| > 3\sigma(|F_o|)$ (R_F 4.3% for those 2775 data with $|F_o| > 6\ \sigma(|F_o|)$). The central iridium atom has a distorted trigonal bipyramidal coordination geometry in which the methoxy group (Ir–OMe 2.057(8) Å) and carbonyl ligand (Ir–CO 1.897(14) Å) occupy axial sites with ∠MeO–Ir–CO 174.7(4)°. The two triphenylphosphine ligands occupy equatorial sites (Ir–P(1) 2.399(3), Ir–P(2) 2.390(3) Å, ∠P(1)–Ir–P(2) 110.32(11)°) and the TCNE ligand is linked in an η^2 "face-on" fashion with the olefinic bond parallel to the equatorial coordination plane (Ir–C(4) 2.176(10), Ir–C(7) 2.160(12) Å) and lengthened substantially from its value in the free olefin (C(4)–C(7) 1.539(17) Å).

Introduction

The coordination of alkenes to transition metal ions causes activation of the C=C bond and is important in many catalytic cycles [1,2]. Thus, the Wacker process (for the production of acetaldehyde from ethylene and dioxygen) involves the coordination of ethylene to palladium with subsequent attack on the ethylene by OH^- from a position external to the metal atom's coordination sphere [3,4]. The reaction does not involve migration of OH^- within the coordination sphere of the palladium atom, nor does it result from insertion of ethylene into a Pd–O bond. The detailed

0022-328X/87/$03.50

stereochemistry of the Wacker process has been established from labelling studies utilizing CHD=CHD [3,4].

We have shown recently that the carbonylation of *trans*-$ROIr(CO)(PPh_3)_2$ to the carboalkoxy product $ROC(O)Ir(CO)_2(PPh_3)_2$ occurs via the external attack of OR^- on a coordinated carbonyl ligand [5,6]. The addition of an alkoxide to an alkene is an important step in the carboalkoxylation of alkenes on palladium catalysts [7–12]. The typical reaction conditions render it difficult to distinguish between internal (*endo*) attack or external (*exo*) attack, but it is generally assumed that external attack occurs in this case too, by analogy with the Wacker process [12].

The above considerations led us to believe that complexes with both metal–alkoxide and metal–alkene linkages (hereafter termed alkoxy-alkene complexes) might well be stable, although (to the best of our knowledge) no such species have previously been reported. In this manuscript we report some reactions of alkenes with selected *trans*-$ROIr(CO)(PPh_3)_2$ species and the crystal structure of one alkoxy-alkene product, $MeOIr(CO)(PPh_3)_2(TCNE)$ (TCNE = tetracyanoethylene).

Experimental

Iridium trichloride, $IrCl_3 \cdot xH_2O$, was loaned by Johnson Matthey Inc. All solvents were dried and degassed prior to use. All syntheses were accomplished under a nitrogen or argon atmosphere. Infrared spectra were recorded on a Beckman 4240, and ^1H NMR and ^{31}P NMR spectra were recorded on a Varian EM390 or on a JEOL FX90Q.

Preparation of $MeOIr(CO)(PPh_3)_2(TCNE)$

In a dry-box, a solution of 0.10 g *trans*-$MeOIr(CO)(PPh_3)_2$ [13] in 10 ml benzene was treated with 0.02 g tetracyanoethylene (TCNE) in benzene. After stirring for 10 min, the resulting precipitate was filtered and washed once with benzene and twice with hexanes. Further purification of the solid was accomplished by preparing a saturated solution of the solid in THF and adding to it hexanes (twice the volume of the solution). After stirring for 10 min a yellow precipitate was filtered and washed with hexanes. IR in CH_2Cl_2 showed ν(CO) 2038 and ν(CN) 2228 cm^{-1}. ^1H NMR in CD_2Cl_2 showed 2.89 (s) and 7.0 ppm (m); ^{31}P NMR in CD_2Cl_2/CH_2Cl_2 (^1H NMR decoupled) showed −11.33 ppm(s). Crystals suitable for crystallographic analysis were grown by slow diffusion of pentane into a saturated solution of the solid in CH_2Cl_2/CCl_4. Microanal. Found: C, 57.14; H, 3.81; P, 6.80. calc: C, 58.46; H, 3.68; P, 6.85%.

Attempted reaction of trans-$ROIr(CO)(PPh_3)_2$ with ethylene (R = Ph, H)

0.20 g of the iridium complex in 25 ml cyclohexane were placed in a pressure bottle and charged with 3 atm of ethylene. The solution was stirred for several days at room temperature and monitored by IR. No obvious reaction occurred after three days so the solution was heated (65 °C). No reaction was evident after 1 week.

Reaction of trans-$MeOIr(CO)(PPh_3)_2$ with dimethyl maleate

In a glovebox 0.10 g of *trans*-$MeOIr(CO)(PPh_3)_2$ was dissolved in 10 ml benzene. 2.25 ml of dimethyl maleate (DMM) were added to the solution (a 140-fold excess). The solution was stirred for 3 h (the disappearance of starting material was shown

by IR). 20 ml hexanes were added and the flask was sealed, brought out of the glovebox, and placed in a 0 °C bath. After the solution was stirred for 10 min, a cream colored solid precipitated, was filtered, and washed with pentane. A KBr disk of the solid showed IR absorptions at 1993vs, 1708s, 1430s, and 1480m cm^{-1}. A solution IR or NMR was not obtained since the complex dissociates unless a large excess of olefin is present in solution (eq. 1).

$$MeOIr(CO)(PPh_3)_2(DMM) \rightleftharpoons \textit{trans}\text{-}MeOIr(CO)(PPh_3)_2 + DMM \quad (1)$$

Collection of X-ray diffraction data on MeOIr(CO)(PPh$_3$)$_2$(TCNE)

A yellow crystal of approximate dimensions $0.2 \times 0.2 \times 0.3$ mm^3 was sealed in a thin-walled glass capillary, mounted on a eucentric goniometer and centered on a Syntex $P2_1$ four-circle diffractometer. The determination of unit cell dimensions, Bravais lattice type and the crystal's orientation matrix were performed as described previously [14]. The final unit cell parameters are based on a least-squares analysis of 25 reflections (Mo-K_α, $2\theta = 20 \rightarrow 30°$). Intensity data were collected by means of a coupled θ(crystal)–2θ(counter) scan using conditions described in Table 1. The data were corrected for absorption and for Lorentz and polarization effects. Data were placed on an approximately absolute scale by a Wilson plot. The diffraction symmetry was *mmm* (D_{2h}), with the following systematic absences: $0kl$ for $k = 2n + 1$; $h0l$ for $l = 2n + 1$; $hk0$ for $h = 2n + 1$. The crystal can uniquely be assigned to the centrosymmetric orthorhombic space group *Pbca* (No. 61).

TABLE 1

EXPERIMENTAL DATA FOR THE X-RAY DIFFRACTION STUDY OF MeOIr(CO)(PPh$_3$)$_2$(TCNE)

Unit cell data

Crystal system: orthorhombic	$Z = 8$
Space group: *Pbca* (No. 61)	Formula: $C_{44}H_{33}IrN_4O_2P_2$
a 17.806(4) Å	mol. wt: 904
b 20.769(4) Å	D_{calc} 1.58 g cm^{-3}
c 20.589(6) Å	T 24 °C (297 K)
V 7614(3) Å^3	

Collection of X-ray diffraction data

Diffractometer: Syntex $P2_1$

Radiation: Mo-$K_{\bar{\alpha}}$ ($\bar{\lambda}$ 0.710730 Å)

Monochromator: highly oriented (pyrolytic) graphite: equatorial mode with 2θ(m) = 12.160°; assumed to be 50% perfect/50% ideally mosaic for polarization correction.

Reflections meas'd: $+h$, $+k$, $+l$ for $2\theta = 5 \rightarrow 45°$, yielding 5003 unique data; 3502 data with $|F_o| > 3\sigma(|F_o|)$ used in the crystallographic analysis

Scan type: coupled θ(crystal)–2θ(counter)

Scan width: $[2\theta(K_{\alpha_1}) - 0.9]° \rightarrow [2\theta(K_{\alpha_2}) + 0.9]°$

Scan speed: 4.0 deg/min (in 2θ)

Backgrounds: stationary crystal, stationary-counter at the two extremes of the 2θ scan; each for one-quarter of the total scan time.

Standard reflns: three mutually orthogonal reflections collected before each set of 97 data points. No decay observed.

Absorption correction: μ(Mo-K_α) 38.5 cm^{-1}; corrected empirically by interpolation (in 2θ and ϕ) for 3 close-to-axial (ψ-scan) reflections.

TABLE 2

POSITIONAL PARAMETERS FOR MeOIr(CO)(PPh_3)$_2$(TCNE)

Atom	x	y	z	B (Å^2)
Ir	0.05162(2)	0.12142(2)	0.20752(2)	
P(1)	0.06506(18)	0.14496(15)	0.32100(15)	
P(2)	0.00580(18)	0.21375(15)	0.15072(15)	
O(1)	0.16195(47)	0.14371(37)	0.18814(40)	
O(2)	−0.11208(55)	0.08577(43)	0.22062(44)	
N(3)	0.00632(65)	−0.06049(56)	0.25054(67)	
N(5)	0.23151(65)	−0.00751(54)	0.19677(63)	
N(6)	0.16496(63)	0.07764(53)	0.04216(52)	
N(8)	−0.05999(62)	0.00178(52)	0.08511(55)	
C(1)	0.21026(70)	0.18037(64)	0.20975(73)	
C(2)	−0.04966(77)	0.09536(56)	0.21898(59)	
C(3)	0.04519(77)	−0.02484(58)	0.22610(61)	
C(4)	0.09082(68)	0.02305(49)	0.19451(62)	
C(5)	0.17092(69)	0.00754(54)	0.19710(64)	
C(6)	0.12111(73)	0.06608(60)	0.08081(63)	
C(7)	0.06511(60)	0.05263(51)	0.12971(62)	
C(8)	−0.00440(78)	0.02436(61)	0.10367(65)	
C(11)	0.10786(62)	0.22144(55)	0.34465(56)	2.48(24)
C(12)	0.08917(65)	0.27658(58)	0.31038(56)	2.87(26)
C(13)	0.11522(76)	0.33781(66)	0.33165(68)	4.16(31)
C(14)	0.15882(73)	0.34154(64)	0.38608(63)	3.73(29)
C(15)	0.17794(75)	0.28784(72)	0.41964(68)	4.37(32)
C(16)	0.15360(72)	0.22644(63)	0.39949(63)	3.71(29)
C(21)	0.12427(65)	0.08493(57)	0.36401(59)	2.69(25)
C(22)	0.10089(88)	0.06119(76)	0.42349(79)	5.33(37)
C(23)	0.1501(10)	0.01953(84)	0.45659(82)	6.61(42)
C(24)	0.21712(84)	0.00207(75)	0.43119(74)	4.90(34)
C(25)	0.23773(76)	0.02452(67)	0.37389(70)	4.17(31)
C(26)	0.19184(74)	0.06605(68)	0.33833(66)	4.13(31)
C(31)	−0.02201(64)	0.14411(56)	0.36703(58)	2.72(25)
C(32)	−0.04407(69)	0.19498(55)	0.40575(57)	2.96(25)
C(33)	−0.11072(80)	0.19231(69)	0.44122(69)	4.43(33)
C(34)	−0.15772(76)	0.13890(65)	0.43453(64)	4.11(31)
C(35)	−0.13575(72)	0.08819(63)	0.39728(63)	3.62(29)
C(36)	−0.06870(70)	0.08858(60)	0.36420(61)	3.36(28)
C(41)	−0.03888(62)	0.18396(53)	0.07621(53)	2.38(23)
C(42)	0.00179(67)	0.17108(58)	0.01870(58)	2.95(26)
C(43)	−0.03422(69)	0.14303(60)	−0.03466(62)	3.68(29)
C(44)	−0.10833(68)	0.12419(67)	−0.03065(60)	3.64(26)
C(45)	−0.14933(69)	0.13705(58)	0.02481(60)	3.49(28)
C(46)	−0.11498(66)	0.16557(58)	0.07723(59)	2.89(26)
C(51)	−0.07037(61)	0.26294(54)	0.18588(54)	2.64(25)
C(52)	−0.10180(69)	0.31061(60)	0.14649(61)	3.34(28)
C(53)	−0.15906(83)	0.34966(69)	0.17209(72)	4.81(34)
C(54)	−0.18195(71)	0.33883(64)	0.23473(65)	3.91(31)
C(55)	−0.15042(76)	0.29295(65)	0.27331(62)	4.13(31)
C(56)	−0.09351(64)	0.25419(55)	0.24867(61)	2.72(24)
C(61)	0.07804(59)	0.27192(53)	0.12858(55)	2.31(24)
C(62)	0.14039(62)	0.25276(58)	0.09219(56)	2.62(24)
C(63)	0.19663(72)	0.29587(66)	0.07697(64)	3.81(30)
C(64)	0.19108(72)	0.35974(64)	0.09903(63)	4.01(31)
C(65)	0.13089(68)	0.37816(68)	0.13590(60)	3.80(27)
C(66)	0.07347(65)	0.33616(57)	0.14912(58)	2.97(26)

TABLE 2 (continued)

Atom	x	y	z	B (Å^2)
H(1)	0.2573	0.1769	0.1876	6.0
H(2)	0.2206	0.1709	0.2557	6.0
H(3)	0.1948	0.2247	0.2084	6.0
H(12)	0.0579	0.2734	0.2713	6.0
H(13)	0.1013	0.3769	0.3084	6.0
H(14)	0.1769	0.3839	0.4006	6.0
H(15)	0.2078	0.2923	0.4590	6.0
H(16)	0.1692	0.1873	0.4242	6.0
H(22)	0.0509	0.0712	0.4400	6.0
H(23)	0.1358	0.0037	0.4997	6.0
H(24)	0.2498	−0.0285	0.4542	6.0
H(25)	0.2871	0.0118	0.3557	6.0
H(26)	0.2069	0.0811	0.2948	6.0
H(32)	−0.0114	0.2325	0.4085	6.0
H(33)	−0.1243	0.2270	0.4712	6.0
H(34)	−0.2061	0.1373	0.4562	6.0
H(35)	−0.1682	0.0502	0.3949	6.0
H(36)	−0.0534	0.0508	0.3379	6.0
H(42)	0.0552	0.1811	0.0173	6.0
H(43)	−0.0062	0.1370	−0.0748	6.0
H(44)	−0.1319	0.1010	−0.0668	6.0
H(45)	−0.2026	0.1271	0.0275	6.0
H(46)	−0.1431	0.1737	0.1168	6.0
H(52)	−0.0835	0.3160	0.1021	6.0
H(53)	−0.1808	0.3839	0.1444	6.0
H(54)	−0.2223	0.3653	0.2520	6.0
H(55)	−0.1678	0.2871	0.3176	6.0
H(56)	−0.0705	0.2208	0.2750	6.0
H(62)	0.1438	0.2083	0.0771	6.0
H(63)	0.2394	0.2825	0.0515	6.0
H(64)	0.2300	0.3908	0.0877	6.0
H(65)	0.1277	0.4227	0.1521	6.0
H(66)	0.0297	0.3501	0.1736	6.0

Solution and refinement of the structure

All calculations were performed using the SUNY-Buffalo modified version of the Syntex XTL interactive crystallographic program package [15]. Scattering factors for neutral atoms were used in their analytical form [16a]; corrections were made for both the real ($\Delta f'$) and imaginary ($i\Delta f''$) components of anomalous dispersion [16b] for all non-hydrogen atoms. The function minimized during the least-squares procedures was $\Sigma w(|F_0| - |F_c|)^2$ where $1/w = [\sigma(|F_0|)]^2 + [0.015|F_0|]^2$. Discrepancy indices used below are defined in eqs. 2–4. (Here, NO is the number of observations and NV is the number of variables.)

$$R_F(\%) = 100\Sigma||F_0| - |F_c||/\Sigma|F_0| \tag{2}$$

$$R_{wF}(\%) = 100\left[\Sigma w(|F_0| - |F_c|)^2/\Sigma w|F_0|^2\right]^{1/2} \tag{3}$$

$$GOF = \left[\Sigma w(|F_0| - |F_c|)^2/(NO - NV)\right]^{1/2} \tag{4}$$

TABLE 3

ANISOTROPIC THERMAL PARAMETERS FOR MeOIr(CO)$(PPh_3)_2$(TCNE) [a]

Atom	B_{11}	B_{22}	B_{33}	B_{12}	B_{13}	B_{23}
Ir	2.152(19)	1.752(18)	2.084(19)	−0.029(21)	−0.025(21)	0.021(21)
P(1)	2.99(16)	2.55(14)	2.21(14)	0.12(12)	−0.05(13)	−0.00(11)
P(2)	2.84(15)	2.17(14)	2.17(15)	0.31(13)	0.03(13)	0.03(12)
O(1)	3.46(41)	2.33(40)	4.67(52)	0.62(34)	1.07(38)	1.34(34)
O(2)	4.75(51)	3.95(46)	4.40(58)	−0.32(43)	−0.32(46)	0.39(40)
N(3)	4.43(65)	3.93(64)	7.60(82)	−1.70(53)	0.79(62)	2.08(61)
N(5)	4.01(60)	3.69(60)	7.07(84)	1.57(52)	0.19(61)	0.56(61)
N(6)	3.97(58)	4.28(62)	3.36(59)	−0.06(51)	1.69(52)	−0.42(50)
N(8)	3.43(58)	3.80(58)	5.60(68)	−0.83(52)	−0.89(55)	−1.20(51)
C(1)	3.50(67)	3.75(68)	4.95(76)	−0.64(58)	−1.29(70)	1.66(69)
C(2)	3.41(63)	2.84(55)	2.87(66)	0.38(58)	−0.23(63)	−0.13(47)
C(3)	4.04(67)	2.27(56)	4.20(76)	−0.22(60)	−0.33(64)	0.22(50)
C(4)	4.08(61)	0.25(44)	4.33(75)	0.07(45)	0.35(56)	0.16(47)
C(5)	3.18(63)	1.93(55)	3.88(74)	1.45(50)	−0.12(60)	−0.28(53)
C(6)	3.32(67)	2.55(62)	2.76(67)	0.36(54)	−0.01(58)	−0.94(53)
C(7)	1.60(54)	1.61(51)	4.29(67)	0.99(44)	−0.60(51)	−0.94(49)
C(8)	4.11(75)	2.37(63)	3.81(72)	−0.22(58)	−0.15(63)	−0.20(56)

[a] The anisotropic thermal parameters are in standard XTL format and enter the expression for the calculated structure factor in the form: $\exp[-0.25(h^2a^{*2}B_{11} + k^2b^{*2}B_{22} + l^2c^{*2}B_{33} + 2hka^*b^*B_{12} + 2hla^*c^*B_{13} + 2klb^*c^*B_{23})]$.

The position of the iridium atom was determined from a Patterson map. All remaining non-hydrogen atoms were located from a difference-Fourier synthesis. All hydrogen atoms were placed in calculated positions, each with an idealized C–H distance of 0.95 Å [17]. Refinement of positional and thermal parameters (isotropic for carbon atoms of the PPh_3 ligands and anisotropic for all other non-hydrogen atoms) converged with R_F 6.2% and R_{wF} 5.0% for those 3502 data with $|F_0| > 3\sigma(|F_0|)$ (R_F 4.3%, R_{wF} 4.2% for those 2775 data with $|F_0| > 6\sigma(|F_0|)$).

A final difference-Fourier synthesis revealed no remaining significant features; the structure is thus both correct and complete. Positional and thermal parameters are collected in Tables 2 and 3.

Results and discussion

Activated alkenes add to the 16-electron alkoxy complexes, *trans*-ROIr(CO)-$(PPh_3)_2$, at ambient temperatures or below, to yield 18-electron adducts (eq. 5).

$$\textit{trans}\text{-ROIr(CO)}(PPh_3)_2 + \text{alkene} \rightarrow \text{ROIr(CO)}(PPh_3)_2(\text{alkene}) \quad (5)$$

A stable adduct is formed with alkene = TCNE, but the adduct for alkene = DMM is stable only in the presence of a large excess of DMM ($K = 4\ M^{-1}$). No evidence of adduct formation is observed for C_2H_4. (Under conditions which might force the reaction, the complex *trans*-MeOIr(CO)$(PPh_3)_2$ decomposes [13]. We utilized both *trans*-HOIr(CO)$(PPh_3)_2$ and *trans*-PhOIr(CO)$(PPh_3)_2$ under more forcing conditions but still found no evidence of reaction with C_2H_4.)

The observed trend in the stability of alkene adducts (viz. TCNE > DMM > C_2H_4) is similar to that observed for adducts of Vaska's complex, *trans*-

$Ir(CO)(PPh_3)_2Cl$, and is consistent with electron acceptance by the alkene (i.e., d_π–$\pi^\star$ metal → alkene back-donation) as the dominant stabilizing force [18]. The effect of the ligand X on the stability of $XIr(CO)(PPh_3)_2$(alkene) complexes (X = Me > Cl > OMe) is also consistent with the importance of d_π–$\pi^\star$ back-donation to the olefin.

Spectroscopic studies do not provide unambiguous information on the structure of these alkene complexes. The carbonyl stretching frequency shows a large shift to higher frequency upon adduct formation, with the magnitude of the shift being dependent upon the π-acceptor capability of the alkene. Thus, ν(C≡O) 2038 cm^{-1} for $MeOIr(CO)(PPh_3)_2$(TCNE) and 1993 cm^{-1} for $MeOIr(CO)(PPh_3)_2$(DMM). These results are similar to those observed for adducts of Vaska's complex [18]. NMR spectra of $MeOIr(CO)(PPh_3)_2$(TCNE) show the presence of the methoxy group (δ 2.89(s) ppm) and the equivalence of the PPh_3 ligands (the ^{31}P NMR spectrum consists of a singlet).

In no case have we observed an insertion/migration with the alkoxide moiety linking to the alkene fragment. When CO is added to *trans*-$MeOIr(CO)(PPh_3)_2$, it is a sufficiently strong ligand to displace methoxide, which then attacks the carbon atoms of a coordinated CO ligand, producing, finally, $MeOC(O)Ir(CO)_2(PPh_3)_2$ [5,6,19]. The weaker alkene ligand (vis á vis CO) evidently cannot displace OMe^- by a similar reaction pathway.

We have determined the crystal structure of $MeOIr(CO)(PPh_3)_2$(TCNE) to ascertain its stereochemistry and, in particular, to determine the relative positions of alkene and alkoxy ligands.

Description of the molecular structure of $MeOIr(CO)(PPh_3)_2$(TCNE)

The crystal contains an ordered arrangement of discrete molecular units of $MeOIr(CO)(PPh_3)_2$(TCNE) separated by normal Van der Waals' distances. There are no abnormally short intermolecular contacts. The overall geometry and labelling

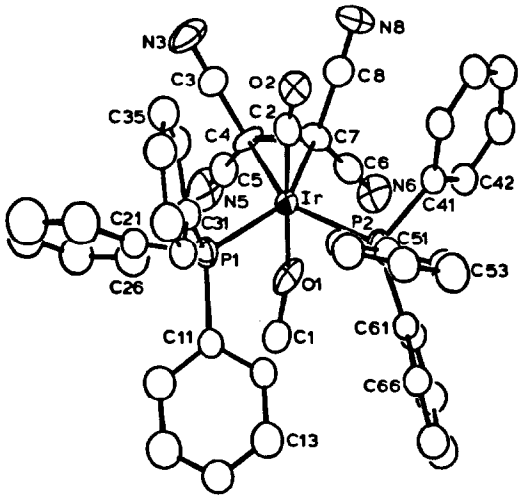

Fig. 1. Labelling of atoms and molecular geometry for $MeOIr(CO)(PPh_3)_2$(TCNE). [ORTEP diagrams; 30% probability contours.]

TABLE 4

INTERATOMIC DISTANCES (Å) FOR $MeOIr(CO)(PPh_3)_2(TCNE)$

(A) Ir – ligand distances			
Ir–P(1)	2.399(3)	Ir–P(2)	2.390(3)
Ir–O(1)	2.057(8)	Ir–C(2)	1.897(14)
O(1)–C(1)	1.232(15)	C(2)–O(2)	1.130(17)
Ir–C(4)	2.176(10)	Ir–C(7)	2.160(12)
Ir–cent [a]	2.027		
(B) Phosphorus – carbon distances			
P(1)–C(11)	1.828(12)	P(2)–C(41)	1.836(11)
P(1)–C(21)	1.858(12)	P(2)–C(51)	1.846(11)
P(1)–C(31)	1.817(12)	P(2)–C(61)	1.822(11)
(C) Distances within the TCNE ligand			
C(4)–C(3)	1.439(17)	C(3)–N(3)	1.131(18)
C(4)–C(5)	1.463(17)	C(5)–N(5)	1.123(17)
C(7)–C(6)	1.444(17)	C(6)–N(6)	1.140(17)
C(7)–C(8)	1.471(17)	C(8)–N(8)	1.160(18)
C(4)–C(7)	1.539(17)		
(D) Distances in the PPh_3 ligands			
C(11)–C(12)	1.386(16)	C(41)–C(42)	1.413(16)
C(12)–C(13)	1.423(18)	C(42)–C(43)	1.399(17)
C(13)–C(14)	1.366(19)	C(43)–C(44)	1.379(17)
C(14)–C(15)	1.365(20)	C(44)–C(45)	1.381(17)
C(15)–C(16)	1.409(20)	C(45)–C(46)	1.375(17)
C(16)–C(11)	1.396(17)	C(46)–C(41)	1.408(16)
C(21)–C(22)	1.384(20)	C(51)–C(52)	1.397(17)
C(22)–C(23)	1.407(24)	C(52)–C(53)	1.405(19)
C(23)–C(24)	1.353(23)	C(53)–C(54)	1.371(20)
C(24)–C(25)	1.320(21)	C(54)–C(55)	1.362(19)
C(25)–C(26)	1.396(19)	C(55)–C(56)	1.390(18)
C(26)–C(21)	1.372(18)	C(56)–C(51)	1.369(17)
C(31)–C(32)	1.381(16)	C(61)–C(62)	1.397(16)
C(32)–C(33)	1.394(19)	C(62)–C(63)	1.379(17)
C(33)–C(34)	1.396(20)	C(63)–C(64)	1.406(19)
C(34)–C(35)	1.360(19)	C(64)–C(65)	1.368(18)
C(35)–C(36)	1.374(18)	C(65)–C(66)	1.371(17)
C(36)–C(31)	1.423(17)	C(66)–C(61)	1.402(16)

[a] cent is the midpoint of the C(4)–C(7) bond.

scheme are shown in Fig. 1. Interatomic distances and angles are contained in Tables 4 and 5.

The central iridium atom has a distorted trigonal bipyramidal coordination geometry, as shown in Fig. 2. The carbonyl ligand (C(2)–O(2)) and the methoxy ligand (O(1)–C(1)) occupy axial sites with a *trans* angle of C(2)–Ir–O(1) 174.71(44)°. The carbonyl ligand is close to linear with Ir–C(2)–O(2) 171.5(11)°, while the iridium-methoxide system is bent with Ir–O(1)–C(1) 137.4(9)°. The two triphenylphosphine ligands and the TCNE ligand ("cent" is the midpoint at the originally olefinic (C(4)–C(7)) bond) occupy equatorial sites, with angles P(1)–Ir–P(2) 110.32(11), P(1)–Ir–cent 126.92 and P(2)–Ir–cent 122.72°. The axial-equatorial angles are in the range 83–93°. Angles involving the carbonyl ligand, C(2)–O(2), are: P(1)–Ir–C(2) 91.85(39); P(2)–Ir–C(2) 87.99(39) and C(2)–Ir–cent 91.89°.

(Continued on p. 255)

TABLE 5. INTERATOMIC ANGLES (°) FOR $MeOIr(CO)(PPh_3)_2(TCNE)$

(A) Angles about the iridium atom			
P(1)–Ir–P(2)	110.32(11)	O(1)–Ir–C(2)	174.71(44)
P(1)–Ir–O(1)	92.72(24)	O(1)–Ir–cent	83.24
P(1)–Ir–C(2)	91.85(39)	C(2)–Ir–cent	91.89
P(1)–Ir–cent	126.92	C(2)–Ir–C(4)	93.01(49)
P(1)–Ir–C(4)	106.22(32)		
P(1)–Ir–C(7)	147.79(31)		
P(2)–Ir–O(1)	92.91(24)	C(2)–Ir–C(7)	90.52(48)
P(2)–Ir–C(2)	87.99(39)	O(1)–Ir–C(4)	83.16(38)
P(2)–Ir–cent	122.72	O(1)–Ir–C(7)	84.20(38)
P(2)–Ir–C(4)	143.40(32)	C(7)–Ir–C(4)	41.57(43)
P(2)–Ir–C(7)	101.87(31)		
(B) Ir–P–C and C–P–C angles			
Ir–P(1)–C(11)	118.58(39)	C(11)–P(1)–C(21)	102.68(53)
Ir–P(1)–C(21)	112.60(39)	C(11)–P(1)–C(31)	103.01(53)
Ir–P(1)–C(31)	114.87(40)	C(21)–P(1)–C(31)	103.25(54)
Ir–P(2)–C(41)	106.66(37)	C(41)–P(2)–C(51)	101.28(51)
Ir–P(2)–C(51)	120.21(38)	C(41)–P(2)–C(61)	108.69(51)
Ir–P(2)–C(61)	114.41(37)	C(51)–P(2)–C(61)	104.45(51)
(C) Ir–C–O and Ir–O Me angles			
Ir–C(2)–O(2)	171.5(11)	Ir–O(1)–C(1)	137.4(9)
(D) Angles within the TCNE ligand			
C(4)–C(3)–N(3)	176.6(14)	C(7)–C(6)–N(6)	179.0(14)
C(4)–C(5)–N(5)	175.8(14)	C(7)–C(8)–N(8)	177.9(14)
C(3)–C(4)–C(5)	112.4(10)	C(6)–C(7)–C(8)	113.8(10)
C(3)–C(4)–C(7)	120.0(10)	C(6)–C(7)–C(4)	118.4(10)
C(5)–C(4)–C(7)	114.2(10)	C(8)–C(7)–C(4)	114.0(10)
C(3)–C(4)–Ir	114.3(8)	C(6)–C(7)–Ir	117.8(8)
C(5)–C(4)–Ir	121.0(8)	C(8)–C(7)–Ir	116.2(8)
C(7)–C(4)–Ir	68.7(6)	C(4)–C(7)–Ir	69.8(6)
(E) P–C–C angles			
P(1)–C(11)–C(12)	118.8(9)	P(2)–C(41)–C(42)	122.8(9)
P(1)–C(11)–C(16)	121.6(9)	P(2)–C(41)–C(46)	119.8(9)
P(1)–C(21)–C(22)	119.4(10)	P(2)–C(51)–C(52)	117.3(9)
P(1)–C(21)–C(26)	120.4(10)	P(2)–C(51)–C(56)	121.2(9)
P(1)–C(31)–C(32)	122.4(9)	P(2)–C(61)–C(62)	120.4(8)
P(1)–C(31)–C(36)	119.0(9)	P(2)–C(61)–C(66)	121.0(9)
(F) C–C–C angles within the PPh_3 ligands			
C(16)–C(11)–C(12)	119.4(11)	C(46)–C(41)–C(42)	117.0(10)
C(11)–C(12)–C(13)	120.2(11)	C(41)–C(42)–C(43)	120.1(11)
C(12)–C(13)–C(14)	119.3(12)	C(42)–C(43)–C(44)	120.7(12)
C(13)–C(14)–C(15)	121.0(13)	C(43)–C(44)–C(45)	120.0(12)
C(14)–C(15)–C(16)	121.1(13)	C(44)–C(45)–C(46)	119.8(11)
C(15)–C(16)–C(11)	119.0(12)	C(45)–C(46)–C(41)	122.3(11)
C(26)–C(21)–C(22)	120.2(12)	C(56)–C(51)–C(52)	121.5(11)
C(21)–C(22)–C(23)	117.4(14)	C(51)–C(52)–C(53)	118.8(12)
C(22)–C(23)–C(24)	121.8(16)	C(52)–C(53)–C(54)	118.3(13)
C(23)–C(24)–C(25)	119.7(15)	C(53)–C(54)–C(55)	122.8(13)
C(24)–C(25)–C(26)	121.6(13)	C(54)–C(55)–C(56)	119.6(12)
C(25)–C(26)–C(21)	119.2(12)	C(55)–C(56)–C(51)	119.2(11)
C(36)–C(31)–C(32)	118.5(11)	C(66)–C(61)–C(62)	118.6(10)
C(31)–C(32)–C(33)	120.9(11)	C(61)–C(62)–C(63)	120.9(11)
C(32)–C(33)–C(34)	119.3(13)	C(62)–C(63)–C(64)	119.2(12)
C(33)–C(34)–C(35)	119.9(13)	C(63)–C(64)–C(65)	119.9(12)
C(34)–C(35)–C(36)	121.6(12)	C(64)–C(65)–C(66)	121.1(12)
C(35)–C(36)–C(31)	119.5(11)	C(65)–C(66)–C(61)	120.2(11)

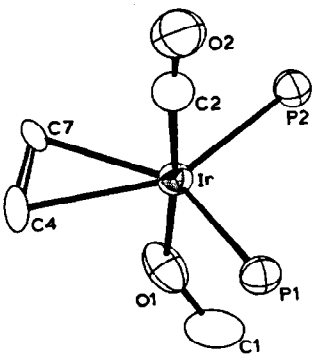

Fig. 2. The coordination sphere of the iridium atom, showing the bending of the methoxy ligand (O(1)–C(1)) away from the TCNE ligand (C(4)–C(7)).

TABLE 6

SELECTED PLANES WITHIN THE $MeOIr(CO)(PPh_3)_2(TCNE)$ MOLECULE [a]

Atom	Dev. (Å)	Atom	Dev. (Å)
(A) The Ir–C(4)–C(7) plane			
$(0.9269X + 0.3381Y - 0.1627Z - 1.0107 = 0)$			
Ir*	0.000	P(1)	0.008
C(4)*	0.000	P(2)	0.082
C(7)*	0.000	O(1)	2.042
		C(2)	−1.893
(B) The C(3) · · · C(5) · · · C(6) · · · C(8) plane			
$(0.1882X - 0.8666Y - 0.4621Z + 1.4957 = 0)$			
C(3)*	−0.057	C(4)	−0.465
C(5)*	0.058	C(7)	−0.468
C(6)*	−0.057	Ir	−2.491
C(8)*	0.056		
(C) The $(NC)_2$ C(4) plane			
$(-0.1033X - 0.4812Y - 0.8705Z + 3.8940 = 0)$			
N(3)*	−0.004		
C(3)*	0.006		
C(4)*	0.010		
C(5)*	−0.029		
N(5)*	0.016		
(D) The $(NC)_2$ C(7) plane			
$(-0.3844X + 0.9158Y - 0.1165Z - 0.2420 = 0)$			
N(6)*	0.004		
C(6)*	−0.008		
C(7)*	0.002		
C(8)*	0.003		
N(8)*	−0.002		
Interplanar angles (°)			
Ir–C(4)–C(7) | C(3) · · · C(5) · · · C(6) · · · C(8)	92.48		
$(NC)_2C(4)$ | $C(7)(CN)_2$	107.43		

[a] Atoms used in the calculation of a plane are marked with an asterisk. Equations of planes are in orthonormalized (Å) coordinates.

Those involving the oxygen of the methoxy group (O(1)) are P(1)–Ir–O(1) 92.72(24), P(2)–Ir–O(1) 92.91(24) and O(1)–Ir–cent 83.24°.

The equatorial alkene ligand is in a parallel configuration with an η^2-"face-on" orientation. The metal–olefin bonding plane as defined by Ir–C(4)–C(7) makes an angle of 92.48° with atoms C(3) · · · C(5) · · · C(6) · · · C(8) of the TCNE ligand (see Table 6). The TCNE ligand is non-planar with the planes of the two $C(CN)_2$ fragments defining a dihedral angle of 107.43° (cf. 180° in non-coordinated TCNE). The iridium–carbon distances are Ir–C(4) 2.176(10), Ir–C(7) 2.160(12), and Ir–cent 2.027 Å. The original carbon–carbon double bond is lengthened from 1.355(2) Å in the parent TCNE molecule [20] to C(4)–C(7) 1.539(17) Å in the present complex. This activation from a normal C=C double bond length to a value more characteristic of a C–C single bond is typical of coordinated TCNE. For example, the central carbon–carbon distance for the TCNE ligand in $Ir(C_6N_4H)(CO)(PPh_3)_2$(TCNE) is 1.526(12) Å [21]; in $IrBr(CO)(PPh_3)_2$(TCNE) it is 1.507(15) Å [22], while for $Ni[CN(t\text{-}Bu)]_2$(TCNE) it is 1.476(5) Å [23]. C–CN bond lengths in the present complex range from 1.439(17) through 1.471(17) Å, averaging 1.454 ± 0.015 Å, cf. 1.431(1) Å in TCNE itself; C≡N bond lengths in the complex range from 1.123(17) through 1.160(18) Å, averaging 1.139 ± 0.016 Å, cf. 1.160(1) Å in TCNE [20].

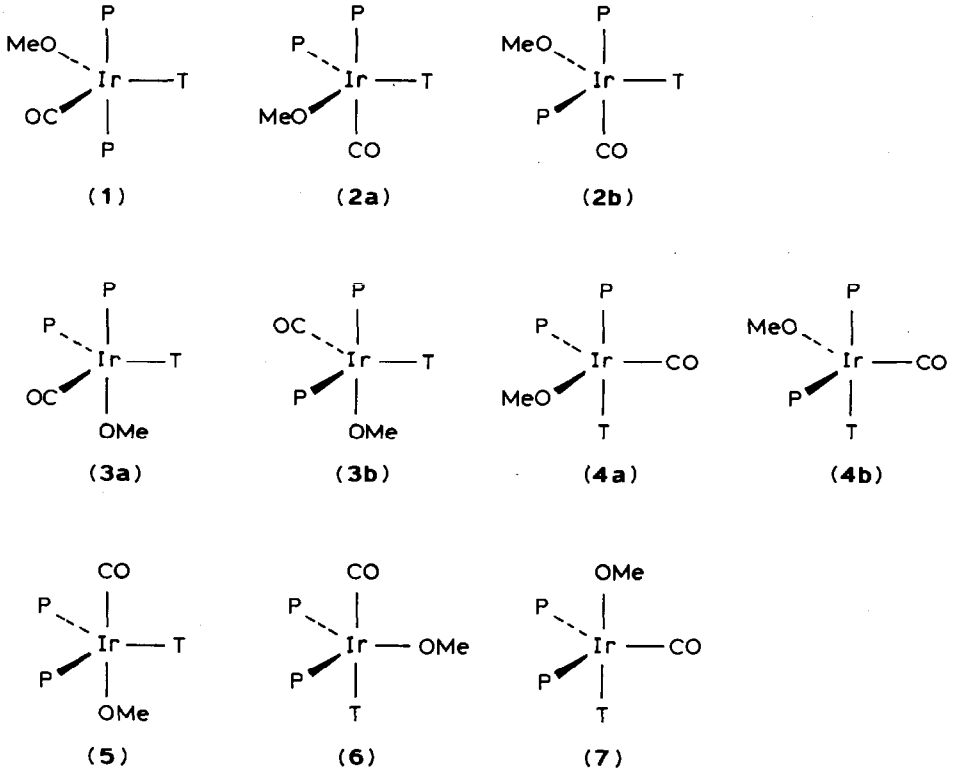

SCHEME 1. Possible isomers of trigonal-bipyramidal $MeOIr(CO)(PPh_3)_2$(TCNE) (P = PPh_3, T = TCNE).

As we have pointed out previously [19], the number of diastereomers of a trigonal bipyramidal complex may be determined simply by the number of permutations of pairs of ligands that can be assigned to the axial positions. For the present complex $MeOIr(CO)(PPh_3)_2(TCNE)$ there are seven possible diastereomers. Four are of idealized C_s symmetry (see **1, 5, 6, 7** of Scheme 1), while three have only C_1 symmetry and give rise to enantiomeric pairs (**2a** and **2b, 3a** and **3b, 4a** and **4b**). Shapley and Osborn have found [24] and Rossi and Hoffmann [25] have shown theoretically that good σ-donors tend to occupy axial sites and that good π-acceptors tend to occupy equatorial sites. However, these tendencies are not absolute and will compete with steric factors. The observed structure of $MeOIr(CO)(PPh_3)_2$-(TCNE) corresponds to **5** in Scheme 1, with the σ-donor methoxy ligand in an axial site, the π-acceptor TCNE ligand in an equatorial site and the two bulky PPh_3 ligands in equatorial sites.

Finally, we note that the Ir–PPh_3 bond lengths are Ir–P(1) 2.399(3) and Ir–P(2) 2.390(3) Å (average = 2.395 ± 0.006 Å) and slightly longer than those found in the analogous five coordinate alkyl-alkene species $MeIr(CO)(PPh_3)_2(MeO_2CCH{=}CHCO_2Me)$ [26], in which Ir–PPh_3 2.344(2) and 2.376(2) Å (average 2.360 ± 0.023 Å).

Supplementary Material Available

A table of amplitudes is available upon request from one of us (M.R.C.).

Acknowledgement

We acknowledge the National Science Foundation and the donors of the Petroleum Research Fund, administered by the American Chemical Society, for partial support of this research. J.D.A. acknowledges the Alfred P. Sloan Foundation for a fellowship. A loan of $IrCl_3 \cdot xH_2O$ was generously provided by Johnson Matthey Corp.

References

1 G.W. Parshall, Homogeneous Catalysis, John Wiley and Sons, New York, 1980.
2 G. Henrici-Olive and S. Olive, Coordination and Catalysis, Verlag Chemie, Weinheim, 1977.
3 J.K. Stille and R. Divakaruni, J. Organomet. Chem., 169 (1979) 239.
4 J.E. Backvall, B. Akermark and S.O. Ljunggren, J. Am. Chem. Soc., 101 (1979) 2411.
5 W. Rees and J.D. Atwood, Organometallics, 4 (1985) 402.
6 W. Rees, M.R. Churchill, J.C. Fettinger and J.D. Atwood, Organometallics, 4 (1985) 2179.
7 R.F. Heck, J. Am. Chem. Soc., 94 (1972) 2712.
8 D.M. Fenton and P.J. Steinward, J. Org. Chem., 37 (1972) 2034.
9 R.F. Heck, 'Organotransition Metal Chemistry', Academic Press, New York, 1974, p. 233.
10 T. Fuchikama, K. Ohishi and I. Ojima, J. Org. Chem., 48 (1983) 3803.
11 H. Alper, B. Despeyroux and J. Woell, Tetrahedron Lett., (1983) 5691.
12 P. Pino, F. Piacenti and M. Bianchi in I. Wender and P. Pino (Eds.) Organic Synthesis via Metal Carbonyls, Vol. 2, John Wiley and Sons, New York, 1977.
13 K.A. Bernard, W. Rees and J.D. Atwood, Organometallics, 5 (1986) 390.
14 M.R. Churchill, R.A. Lashewycz and F.J. Rotella, Inorg. Chem., 16 (1977) 265.
15 Syntex XTL Operations Manual, 2nd Edition, Syntex Analytical Instruments, Inc., Cupertino, Calif., 1976.
16 International Tables for X-ray Diffraction, Vol. 4, Kynoch Press, Birmingham, England, 1974 (a) pp. 99–101, (b) 149–150.

17 M.R. Churchill, Inorg. Chem., 12 (1973) 1213.
18 L. Vaska, Acc. Chem. Res., 1 (1968) 335.
19 M.R. Churchill, J.C. Fettinger, W.M. Rees and J.D. Atwood, J. Organomet. Chem., 304 (1986) 227.
20 P. Becker, P. Coppens and F.K. Ross, J. Am. Chem. Soc., 95 (1973) 7604.
21 J.S. Ricci and J.A. Ibers, J. Am. Chem. Soc., 93 (1971) 2391.
22 J.A. McGinnety and J.A. Ibers, Chem. Commun., (1968) 235.
23 J.K. Stalick and J.A. Ibers, J. Am. Chem. Soc., 92 (1970) 5333.
24 J.R. Shapley and J.A. Osborn, Acc. Chem. Res., 6 (1973) 305.
25 A.R. Rossi and R. Hoffmann, Inorg. Chem., 14 (1975) 365.
26 M.R. Churchill, J.C. Fettinger, W.M. Rees and J.D. Atwood, J. Organomet. Chem., 301 (1986) 99.